Regenerative Engineering and Translational Medicine
https://doi.org/10.1007/s40883-025-00464-3

ORIGINAL RESEARCH

Hypoxia Longitudinally Correlates with Initial Extrinsic and Subsequent Intrinsic Vascularization of Collagen Elastin Matrix-Embedded Arteriovenous Loops in Experimental Rats

Nina Hildenbrand[1,2] · Benjamin Thomas[1] · Florian Falkner[1] · Matthias Schulte[1] · Sebastian Mueller[3,4] · Manfred Jugold[5] · Boyan K. Garvalov[6] · Arno Dimmler[7] · Volker J. Schmidt[8] · Jonathan P. Sleeman[6,9] · Ulrich Kneser[1] · Wilko Thiele[6]

Received: 5 February 2025 / Revised: 30 June 2025 / Accepted: 11 July 2025

Abstract

Purpose Tissue engineering techniques that allow the growth of vascularized tissue are currently being developed and characterized with the help of animal models such as the rat arteriovenous loop (AVL), a microvascular vessel loop that is generated microsurgically, and implanted within an isolation chamber. Inside the chamber, the loop can be embedded in different matrices that become considerably vascularized with time. While vascularization of rat AVLs has been studied in the context of various matrix materials, hypoxia and subsequent vascularization have so far not been longitudinally assessed in rat AVL constructs embedded in a collagen elastin matrix. This assessment, however, is important to determine the peak of vascularization and thus the ideal time frame for transplantation.

Methods We employed histological and micro-computed tomography analyses with subsequent region-based image segmentation that allows three-dimensional reconstruction of the vascular network 5, 15, 21, and 28 days post collagen elastin matrix-embedded AVL generation in rats.

Results The number of newly formed vessels was substantially increased on day 15 compared to day 5 and plateaued at day 21 after surgery. The proportion of hypoxic cells in the loop constructs plateaued at day 15 and correlated significantly with the number of newly formed vessels. Moreover, vascularization was initiated extrinsically at the chamber entrance, and intrinsic sprouting occurred only later.

Conclusion Hypoxia contributes to the vascularization of collagen elastin matrix-embedded AVLs, and extrinsic vascularization can occur through the isolation chamber entrance.

Lay Summary Tissue survival after transplantation strongly depends on blood supply. Therefore, tissue engineering techniques that allow the growth of pre-vascularized tissue hold the promise to find application in reconstructive surgery. Here, we examined vascularization of a collagen-embedded rat arteriovenous loop (AVL) over time. We found that vessel numbers were substantially increased 15–21 days after AVL generation, suggesting that this may be a suitable time frame for

✉ Wilko Thiele
wilko.thiele@medma.uni-heidelberg.de

1 Department of Hand, Plastic and Reconstructive Surgery, Burn Center, BG Trauma Center Ludwigshafen, University of Heidelberg, Ludwigshafen, Germany

2 Department of Orthopedics, Heidelberg University Hospital, Heidelberg, Germany

3 Max Planck Institute for Biological Cybernetics, High-Field Magnetic Resonance Center, Tübingen, Germany

4 Division of Medical Physics in Radiology, German Cancer Research Center (DKFZ), Heidelberg, Germany

5 Small Animal Imaging Center, German Cancer Research Center (DKFZ), Heidelberg, Germany

6 Department of Microvascular Biology and Pathobiology, European Center for Angioscience (ECAS), Medical Faculty Mannheim, University of Heidelberg, TRIDOMUS-Gebäude Haus C, Ludolf-Krehl-Str. 13 - 17, 68167 Mannheim, Germany

7 Institute of Pathology, Vincentius Kliniken Karlsruhe, Karlsruhe, Germany

8 Department of Plastic Surgery and Hand Surgery, Kantonsspital St. Gallen, St. Gallen, Switzerland

9 Institute for Biological and Chemical Systems, Karlsruhe Institute of Technology (KIT), Campus North, Karlsruhe, Germany

Published online: 28 July 2025

transplantation. Moreover, we observed a correlation between hypoxia levels and vessel growth within the matrix, supporting the hypothesis that hypoxia plays a pivotal role in stimulating blood vessel outgrowth in the AVL model.

Description of Future Work The rat arteriovenous loop (AVL) is an ideal model to investigate the influence of various matrix materials on vascularization. However, the effects of other matrix materials on hypoxia-induced angiogenesis, and the influence of angiogenesis-promoting factors on vascularization and survival of the AVL construct post-transplantation remain to be investigated.

Graphical Abstract

Created in BioRender. Thiele, W. (2025) https://BioRender.com/es3w7ng

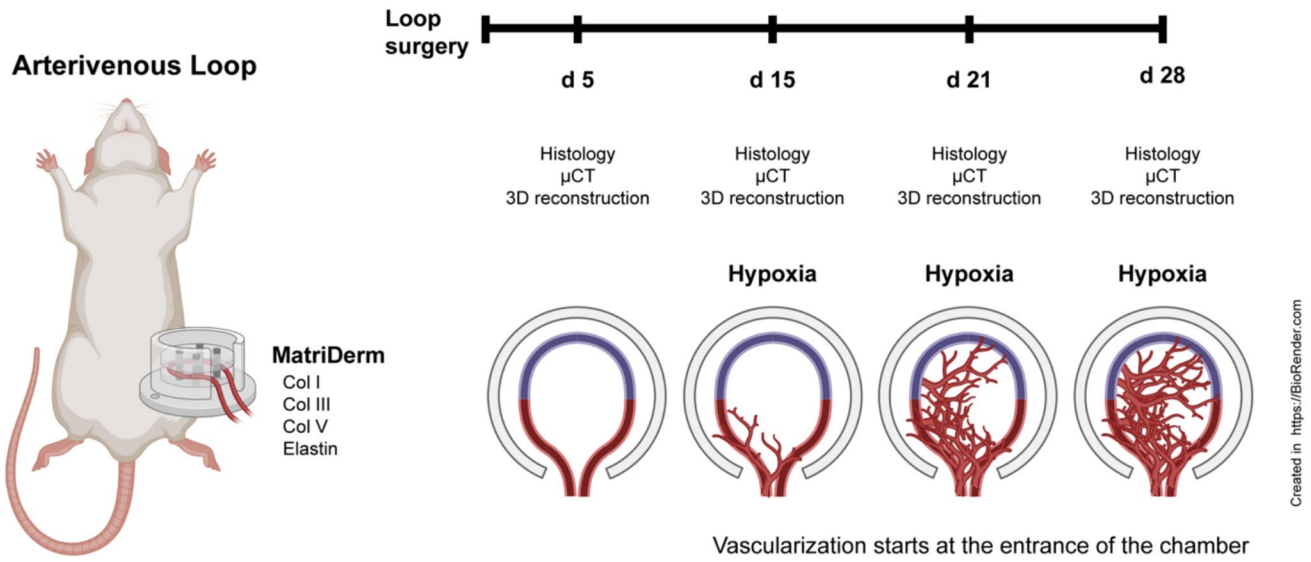

Keywords Tissue engineering · Arteriovenous loop · Collagen elastin matrix · Vascularization · Hypoxia

Abbreviations

AV	Arteriovenous
AVL	Arteriovenous loop
FITC	Fluorescein isothiocyanate
H&E	Hematoxylin and eosin
µCT	Micro-computed tomography
MITK	Medical imaging interaction toolkit
PBS	Phosphate-buffered saline
PFA	Paraformaldehyde
PLGA	Polylactic acid and polyglycolic acid
ROI	Region of interest

Introduction

Tissue engineering techniques hold the promise of producing tissues in vitro or in vivo that can then be implanted into patients in order to repair or replace damaged organs or body parts. The survival of implanted tissues at the recipient site is dependent on a sufficient supply of nutrients and oxygen. Accordingly, in vivo techniques that allow the engineering of vascularized implantable tissue that can be used as pedunculated flap or connected microsurgically to the existing vasculature within the target tissue represent a particularly promising approach. Appropriate in vivo tissue engineering methods that produce vascularized transplantable tissues are currently being developed and characterized preclinically with the help of animal models. An example of such a model is arteriovenous (AV) loops, artificial anastomoses in which a venous graft is positioned between an artery and a vein to form a loop (for a review, see [1]).

The arteriovenous loop (AVL) model has been most intensively studied and characterized in experimental rats, where a venous graft is derived from the saphenous vein and anastomosed between the contralateral saphenous artery and saphenous vein in the medial thigh [2]. The loop can then be placed in a protective chamber that is implanted into the animal. Although an endogenous fibrin matrix develops within the chamber after implantation [3–5], the loops are usually embedded in exogenous biological matrices (e.g. [6–10]). However, certain commonly used matrix materials such as Matrigel or poly-d,l-lactic-co-glycolic acid (PLGA) are immunogenic and therefore have limitations in terms of translatability to clinical application [1, 6, 9] (Table 1). This

Table 1 Comparative overview of four common matrix materials for tissue engineering in the AVL model

Category	Fibrin	PLGA	Matrigel	MatriDerm
Material properties	Protein derived from fibrinogen and thrombin; was first used as matrix in the AVL model and is well-established	Copolymer comprises polylactic acid and polyglycolic acid; composition can be varied to modify material properties	Tumor-derived basement membrane extract; rich in pro-angiogenic growth factors	Bovine-derived acellular collagen-elastin matrix; provides robust mechanical support; relatively novel use as matrix in the AVL model
Vascularization	Early onset: ~ 7 days; vessel sprouting stops early along with the onset of fibrinolysis	Moderate onset: ~ 7–14 days; vessel ingrowth depends on porosity and incorporation of growth factors	Early onset: 3–7 days; high vessel density and sprouting;	Late onset: > 14 days; moderate vessel density; long-term vascular stability
Biodegradability	Rapidly degraded by fibrinolytic enzymes; poor mechanical properties	Variable: Depending on polymer formulation; immunogenic reaction	Rapid: Mostly degraded within 2 weeks	Slow: Partial degradation over several weeks; long-term mechanical stability
Clinical relevance	Clinically applied to improve hemostasis, assist in tissue sealing, and secure sutures in vascular surgery	Clinically used in drug delivery and implants; increased immune reaction/foreign body reaction in tissue engineering	Non-clinical due to murine tumor origin, and variability in composition	Clinically approved for dermal regeneration; suitable scaffold in composite flap engineering and reconstructive surgery
Key references	[1, 4–6, 9]	[1, 6]	[1, 6, 7]	[1, 9]

growing recognition has highlighted the need for improved biomaterials and has led to the increasing adoption of clinically approved matrices such as MatriDerm. MatriDerm is an elastin collagen matrix composed of bovine type I, III, and V collagen fibers and bovine elastin. It is approved for the application in humans and has therefore gained substantial interest as a matrix for tissue engineering purposes [11]. However, given its relatively recent use in the AVL model, the course of vascularization within a MatriDerm matrix remains to be assessed.

The vascularization of rat AVL constructs is driven by hypoxia [4, 7, 12] as well as increased endothelial shear stress due to increased blood flow through the venous graft [8]. Blood flow is a prerequisite for hypoxia-induced angiogenesis [13]. The process of vascularization of AVL constructs has been intensively studied in the context of various matrices such as fibrin [4, 6, 8, 14], Matrigel [6, 7], PLGA [6], and collagen elastin matrices [15] (Table 1). The published data suggests that the onset, speed, and extent of vascularization vary significantly, depending on the matrix material used [6] (Table 1). However, the extent of local hypoxia has so far not been longitudinally assessed and correlated with the extent of vascularization in the context of AVLs embedded in collagen elastin matrices. This assessment, however, is crucial to determine for example the optimal time point for the experimental transplantation of the AVL construct, which might coincide with the vascularization maximum.

We therefore investigated the correlation between hypoxia and vascularization in rat AVLs embedded in a collagen elastin matrix within closed polytetrafluoroethylene ("Teflon") isolation chambers. To this end, we established AVLs in experimental rats. The animals were sacrificed 5, 15, 21, and 28 days after AVL surgery. Vascularization and hypoxia were assessed longitudinally by histology and by region-based image segmentation of micro-computed tomography (μCT) data to allow three-dimensional reconstruction of the vascular network.

Methods

AVL Surgery

All animal experiments were approved by the local regulatory authorities (license numbers: 23 177–07/G13-7–008 and 23 177–07/G15-7–021) and were performed according to German legal requirements.

Rats (Charles River, Sulzfeld, Germany) were kept in groups of 4–5 in type IV Makrolon cages (Tecniplast, Hohenpeißenberg, Germany) containing Abedd Aspen Classic (Ssniff GmbH, Soest, Germany). Rat/mouse extruded food (Ssniff) and fresh water were provided ad libitum.

The room was kept at 22 ± 2 °C and 30–60% humidity on a 8:00–20:00 light cycle. The health status of the animals in the facility is assessed by the supplier (Charles River) before delivery.

Sixteen 7-week-old female Sprague–Dawley rats (271 g +/− 26 SD) were anesthetized with 2% isoflurane. Buprenorphine (0.05 mg/kg, approximately 225 µl/animal s.c.) and heparin (70–80 IE/kg, approximately 2.1 ml/animal i.v.) were applied subcutaneously/intravenously for intraoperative analgesia and to prevent blood clotting, respectively. All surgical procedures were performed by the same microsurgeon using an operative microscope (OPMI pico, Carl Zeiss, Jena, Germany). To isolate the venous graft, an incision of 2–3 cm length was made at the left medial thigh. The left saphenous vein was dissected free from the surrounding connective tissue. The left thigh was then covered with a wet gauze while the contralateral side was prepared. To this end, a 2–3-cm-long incision was made at the right medial thigh. The right saphenous vein and artery were both dissected free from surrounding tissue. The contralateral venous graft was then harvested at a length of approx. 2 cm, flushed with heparin solution, and placed beneath the vessels of the right thigh, and the former proximal end was anastomosed to the artery between the right saphenous vein and artery using interrupted 11–0 Ethilon sutures (Ethicon, Somerville, USA). The AVL was then carefully placed in a polytetrafluoroethylene isolation chamber (custom-manufactured at Karlsruhe Institute of Technology, KIT, Karlsruhe, Germany) between two layers of MatriDerm elastin collagen matrix (Medskin Solutions Dr. Suwelack, Billerbeck, Germany) prepared with 500 µl NaCl solution. The chamber was closed with a matching polytetrafluoroethylene lid and attached to the underlying muscle fascia with a 6–0 suture. Both incision wounds were closed with subcutaneously and intracutaneously-running 4–0 absorbable sutures. For adequate postoperative analgesia, buprenorphine was applied subcutaneously (0.05 mg/kg body weight; approximately 225 µl/animal) twice a day for 2 days.

Pimonidazole Injection, Microfil Injection, and Subsequent Explantation of the Chambers

The polytetrafluoroethylene isolation chambers containing the AVL constructs were explanted 5, 15, 21, and 28 days after surgery, with 4 animals for each time point. Pimonidazole was injected intraperitoneally at 60 mg/kg (approximately 325 µl/animal) into all animals 90 min prior to explantation. Explantation was performed under deep inhalation anesthesia using 2% isoflurane and oxygen and analgesia using buprenorphine (0.05 mg/kg body weight; approximately 225 µl/animal). The abdominal cavity was opened, and the abdominal aorta was then cannulated in a distal direction. Through the aorta, the vascular system of the lower extremities was first flushed with 20 ml of heparin solution (100,000 IE/l) and subsequently with yellow microfil solution (Flow Tec, Inc, Boulder, CA). The afferent saphenous artery and efferent saphenous vein were confirmed to be patent. After homogeneous perfusion of all vessels with 20 ml of microfil solution, the aorta and vena cava were ligated. Euthanasia was then performed by intracardial injection of phenobarbital (16 g phenobarbital in 100 ml solution with 2 ml/kg body weight; approximately 550 µl/animal). For microfil cross-linking, the cadavers were stored for 90 min at 4 °C. After 90 min, isolation chambers with AVL tissue were explanted, fixed in 4% paraformaldehyde (PFA) for 12 h, and stored in phosphate-buffered saline (PBS) solution until µCT scans were performed. The AVL construct of one animal that was sacrificed 15 days post-surgery showed a strong accumulation of granulocytes, indicating inflammation, and was therefore excluded from the study.

µCT and Three-Dimensional Volume Calculation of Vessel Networks

µCT scans were performed with an Inveon small-animal CT (Siemens Healthineers, Erlangen, Germany) at an exposure time of 2000 ms, 17.37 µm slice-thickness, and in-plane resolution of 9.64 µm (Feldkamp Cone Beam). Based on the CT data, the morphology and volume of the vessel networks were evaluated with the 3D region growing tool of MITK (Medical Imaging Interaction Toolkit, dkfz, Heidelberg, Germany) [16]. To this end, a seedpoint was placed in the venous graft, and a threshold interval was defined. The algorithm grew from the seedpoint to neighboring voxels and segmented every voxel within the threshold. The absolute vessel volume was determined by measurement of the completed vessel segmentation. Relative volumes were calculated as the ratio of the volume of the matrix or tissue and the total volume inside the isolation chamber.

Immunohistochemistry and Quantification of Vessels and Hypoxic/Normoxic Cells

After the µCT scans had been performed, the AVL tissues were carefully removed from the isolation chambers and embedded in paraffin. The paraffin blocks were then cut into 5-µm-thick histological sections (Leica RM2255 microtome, Leica Biosystems GmbH, Nussloch, Germany). Immunohistochemistry was performed using a pimonidazole kit (Hypoxyprobe, Inc., Burlington, MA) with anti-pimonidazole mouse IgG1 monoclonal antibody (FITC-MAb1) and rabbit anti-FITC conjugated with horseradish peroxidase as a secondary reagent. The staining was developed by incubation with diaminobenzidine and counterstained with Mayer's hematoxylin. Exemplary sections from each

group of AVL constructs were stained with hematoxylin and eosin (H&E). H&E-stained histological sections were analyzed and photographed with an Olympus BX43 microscope (Olympus Europa SE, Germany). Hypoxyprobe stainings were imaged on an Axio Scan.Z1 slide scanner (Carl Zeiss Microscopy) equipped with a Hitachi HV-F202SCL camera. Selected fields were exported using ZEN software (Zeiss). Microfil-containing vessels and cells were quantified with Fiji/ImageJ (PMID 22743772). The region of interest (ROI) was defined as the region surrounding the venous graft in a vertical section.

Statistics

Plots were generated with Prism Version 8 (GraphPad, Boston, MA). Statistical analysis was performed with Prism Version 8 (GraphPad). Testing for statistical significance was performed via two-way ANOVA with Bonferroni correction (mean vessel number, percentage of hypoxic cells) or Pearson correlation (percentage of hypoxic cells and number of blood vessels). An error probability of < 0.05 was considered statistically significant.

Results

The Number of Newly Formed Vessels Reaches a Maximum at Day 21 After AVL Surgery, While the Total Vessel Volume Steadily Increases Until Day 28 Post-surgery

In order to investigate the development of the vascular network and newly formed vessels in rat AVLs embedded in a collagen elastin matrix over time, we created AVLs in experimental rats and implanted them within polytetrafluoroethylene isolation chambers (Fig. 1a). The AVL constructs were explanted 5, 15, 21, and 28 days post-surgery. The number and volume of the vessels within the chambers, including the main AVL vessels, were analyzed histologically as well

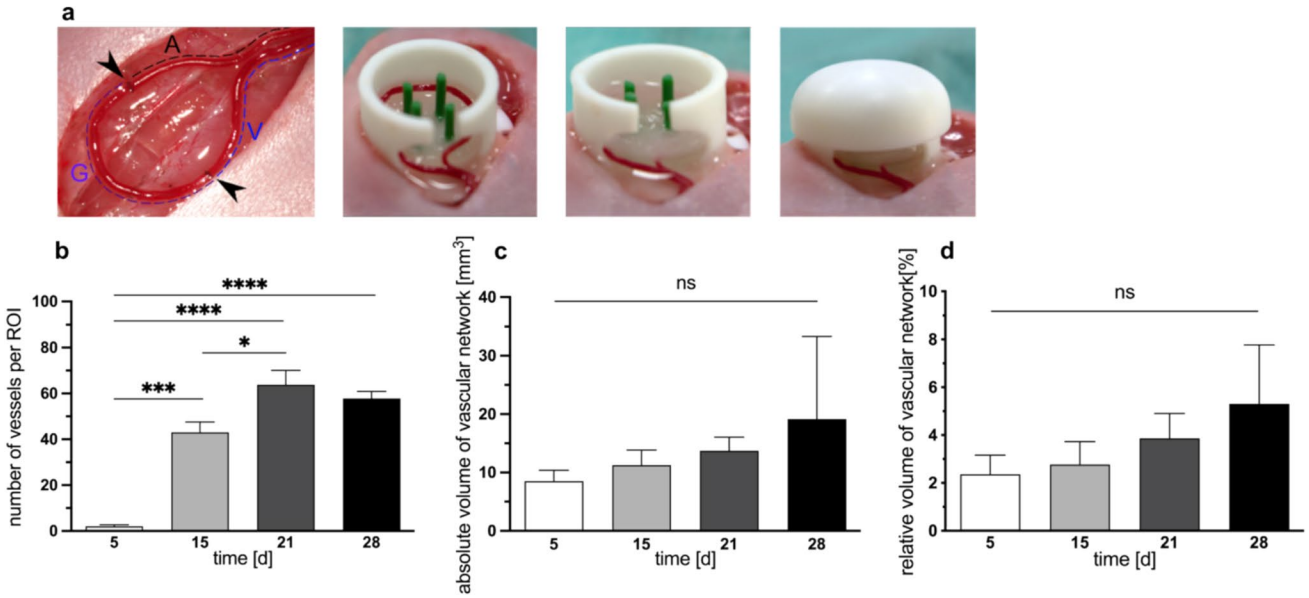

Fig. 1 The number of newly formed vessels in the AVLs is substantially increased 15 days after surgery and reaches a maximum 21 days post-surgery. AVLs were established surgically in 16 experimental rats. The loops were then embedded in a collagen elastin matrix within Teflon chambers that were closed with a lid. Four animals at each time point were sacrificed on day 5, 15, 21, and 28 post-surgery, and the AVL-containing chambers were explanted. The AVL construct of one animal that was sacrificed 15 days post-surgery showed signs of inflammation and was therefore excluded from the study. The AVL constructs were fixed, analyzed via µCT, then carefully removed from the chambers, cut into sections, H&E stained, and analyzed via histology. **a** From left to right: Representative intraoperative images of the AVL (A, saphenous artery; V, saphenous Vein; G, venous graft; arrowheads pointing at the anastomoses); the loop within the chamber on top of the lower MatriDerm layer; AVL embedded between two layers of MatriDerm; chamber with lid. **b** Mean vessel number 5, 15, 21, and 28 days after AVL surgery within a region of interest defined around the AVL vessels. The ROI was consistent throughout all AVL constructs and timepoints. $n = 4$ AVL constructs per group (5, 21, and 28 days post-surgery) and $n = 3$ AVL constructs per group (15 days post-surgery). Error bars represent SE. **c** Absolute volume of the total vascular network in the AVL constructs, determined by µCT and subsequent application of region growing algorithm. $n = 3$ AVL constructs per group. Error bars represent SE. **d** Relative volume of the total vascular network in the AVL constructs, normalized to AVL construct volume, determined by µCT and subsequent application of region growing algorithm. $N = 3$ AVL constructs per group. Error bars represent SE. $^{*}p < 0.05$; $^{***}p < 0.001$; $^{****}p < 0.0001$, ns $p > 0.05$

as by μCT and subsequent application of a region growing algorithm, respectively.

At day 5 post-AVL operation, hardly any newly formed vessels (2.0 ± 0.71) were evident in the AVL construct (Fig. 1b). However, the number of new vessels was substantially and statistically significantly increased at day 15 post-surgery (2.0 ± 0.71 vs. 43.0 ± 4.58; $p = 0.0001$) (Fig. 1b). In comparison to day 15, the number of newly grown vessels was further statistically significantly increased 21 days post-AVL generation, when the vessel counts reached a maximum (43.0 ± 4.58 vs. 63.75 ± 6.26; $p < 0.05$) (Fig. 1b) that remained stable until day 28 post-surgery (57.75 ± 3.12) (Fig. 1b). Moreover, the volume of the vessels within the AVL construct increased steadily from day 5 until day 28 post-surgery (8.52 ± 1.08 vs. 19.16 ± 8.17) (Fig. 1c, d). In addition, we found no signs of hemorrhage in the histological sections, suggesting vascular integrity.

Together, these findings show that vascularization in collagen elastin-embedded rat AVLs starts between 5 and 15 days post-AVL surgery and reaches its maximum 3 weeks after loop surgery.

The Proportion of Hypoxic Cells in Collagen Elastin-Embedded Rat AVL Constructs Is Increased from Day 15 Until Day 28 Post-surgery and Positively and Statistically Significantly Correlates with the Number of Newly Formed Vessels

Hypoxia is one of the most prominent inducers of angiogenesis, and previous reports suggest that hypoxia is a major driving force behind the vascularization of AVL constructs in the rat [4, 7]. In order to investigate the longitudinal development of hypoxia in collagen-elastin-embedded AVLs, we injected pimonidazole into all animals 90 min prior to AV-loop explantation on days 5, 15, 21, and 28 after AVL surgery. The loop constructs were cut into sections that were probed with antibodies specific for pimonidazole. The proportion of hypoxic cells in AVL constructs taken at the time points 5, 15, 21, and 28 days post-AVL surgery was assessed. Endothelial cells of the main AVL vessels were excluded from the analysis.

The percentage of hypoxic cells increased substantially in a statistically significant manner on day 15 post-surgery (23.71 ± 2.06 vs. 71.46 ± 2.25; $p < 0.0001$) and remained at the same elevated level throughout the duration of the experiment until day 28 after surgery (70.90 ± 2.55) (Fig. 2a–e). The increase in the proportion of hypoxic cells coincided with the increase in blood vessel numbers presented above (Fig. 1f), suggesting a possible correlation between hypoxia and the number of newly formed vessels (Fig. 2f). Indeed, Pearson correlation analysis found a significant, positive correlation between the proportion of hypoxic cells and the number of new vessels ($p < 0.05$; $R = 0.88$) (Fig. 2f).

Our findings suggest that hypoxic conditions develop between day 5 and day 15 after AVL surgery and that the outgrowth of new vessels is induced in turn by hypoxia with a slight time lag of approximately 6 days.

Vascularization of AVL Constructs in Closed Isolation Chambers Starts Extrinsically

The findings presented above indicate that hypoxia is induced in the isolation chambers prior to day 5 after AVL surgery and reaches a plateau 10 days later (Fig. 2e). Accordingly, vascularization starts between 5 and 15 days after AVL generation and reaches a maximum 21 days post-surgery. In order to identify and visualize the origin of vascularization and to spatiotemporally follow the vascularization process, we performed region-based three-dimensional image segmentations of μCT scans.

At day 5 post-surgery, hardly any capillary structures were observed in the three-dimensional reconstruction of the AVL, neither inside the chamber, nor at the chamber entrance (Fig. 3a). Ten days later, at day 15 post-surgery, newly formed vessels appeared mainly at the entrance region, both outside, and inside the chamber (Fig. 3b). Since several intermediate-sized vessels are present in the entrance region outside the camber, but not inside the isolation chamber (Fig. 3b), and intermediate-sized vessels need longer to develop than smaller sprouts and capillaries, one can conclude that surprisingly, the sprouts originated from the tissue outside of the chamber and grew along the venous part of the loop, indicating extrinsic vascularization. This observation was consistent among all three available samples explanted 15 days after AVL generation. Extrinsic sprouts were found to subsequently enter the chamber along the arterial part of the loop pedicle at day 21. Intrinsic sprouting could also be observed from day 21 onward, when newly formed vessels emanated mainly from the venous graft portion of the loop, while the arterial portion attached to the graft remained free of sprouts (Fig. 3c). The vessel network inside the chamber had become denser 28 days after AVL generation and remained more pronounced in the venous part and around the graft. Moreover, the graft portion showed dilation, and newly formed vessels were now also visible next to the arterial portion of the loop (Fig. 3d).

Furthermore, the fact that capillaries can be seen in the μCT images is dependent on the presence of and thus successful perfusion with microfil. Therefore, perfusion of the newly formed vessels was also confirmed via μCT.

These data demonstrate that vascularization was initiated extrinsically at the entrance of the isolation chamber between 5 and 15 days after AVL generation, confirming the results obtained from the histological analyses that show a

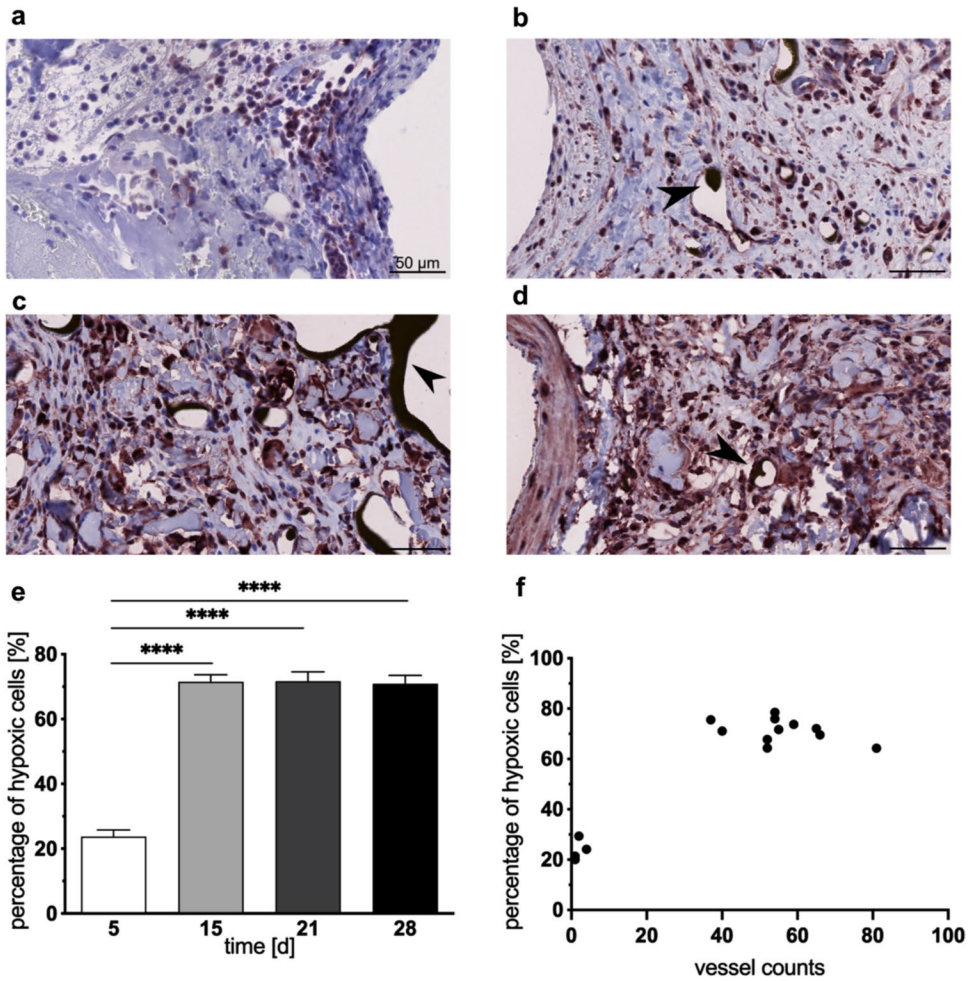

Fig. 2 The percentage of hypoxic cells is increased from day 15 until day 28 post AVL surgery and correlates with the number of blood vessels in the AVL construct. AVLs were established surgically in 16 experimental rats. Pimonidazole was injected into the animals before isolation chamber explantation 5, 15, 21, and 28 days after AVL surgery. The AVL constructs were fixed, then carefully removed from the chambers, and cut into sections. The sections were stained with antibodies specific for pimonidazole. Images were taken, and the proportion of normoxic and hypoxic cells in the AVL constructs relative to total cell numbers (excluding the endothelial cells of the main AVL vessels) was assessed. Representative images of pimonidazole stained vertical sections of AVL constructs at days 5 (**a**), 15 (**b**), 21 (**c**), and 28 (**d**) days after surgery. Scale bars, 50 µm. Arrowheads indicate blood vessels filled with microfil. **e** The percentage of hypoxic cells in relation to total cell counts in the loop constructs at the indicated time points. ****$p < 0.0001$. **f** The percentage of hypoxic cells and the number of newly formed vessels 5, 15, 21, and 28 days after AVL surgery. Pearson correlation analysis of the percentage of hypoxic cells and the number of blood vessels across the four time points of the experiments. $p \leq 0.05$. $R = 0.88$

significant increase in vessel numbers at day 15 (Fig. 1b). Vascularization then continued intrinsically from the venous portion of the loop, the graft, and finally the arterial portion.

Discussion

The reconstruction of extensive soft tissue defects represents a significant challenge in plastic surgery, frequently necessitating the transfer of free tissue flaps for the effective reconstruction of the defect [17–19]. The efficacy of flap transfers is dependent on the presence of adequate vascularization within the flap tissue [18]. Insufficient vascularization frequently results in tissue ischemia and flap failure [20, 21]. Moreover, in order to obtain a flap, a wound of considerable size is generated, and structural weakness of the scar tissue can later lead to abdominal donor site comorbidities [22]. Additionally, in specific scenarios, recipient vessels may be unsuitable for microsurgical anastomoses, such as in patients with peripheral arteriopathy [20].

Tissue engineering techniques represent a viable solution for these challenges, as they facilitate the creation of sufficient recipient vessels [23, 24], and the surgical procedures associated with the establishment and explantation of such tissue engineering constructs are less invasive than flap isolation, and the area of the wound that is inflicted during

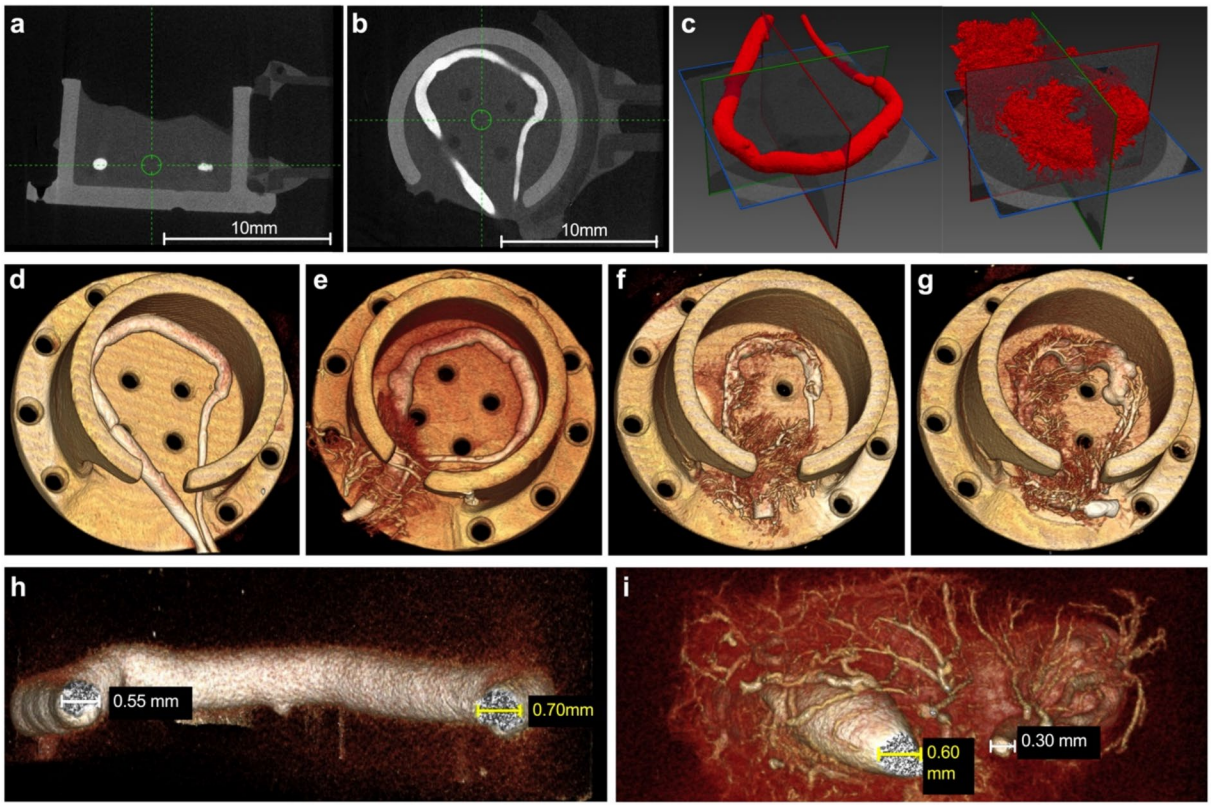

Fig. 3 Vascularization of AVL constructs in closed isolation chambers starts extrinsically between 5 and 15 days post-AVL surgery. AVLs were established surgically in 16 experimental rats. The loops were then embedded in a collagen elastin matrix within Teflon isolation chambers that were closed with a lid. Four animals at each time point were sacrificed on day 5, 15, 21, and 28 post-surgery, and the AVL-containing chambers were explanted. Due to signs of inflammation, one animal that was sacrificed 15 days post-surgery had to be excluded from the study. The AVL constructs were fixed, then analyzed using μCT. Representative coronal (**a**) and axial (**b**) μCT reconstructions of an AVL construct on day 5 are shown. A region-growing algorithm was subsequently applied to quantify vessel volume, with representative results illustrated for days 5 and 28 (**c**). Three-dimensional reconstructions of intrachamber vasculature are presented for days 5 (**d**), 15 (**e**), 21 (**f**), and 28 (**g**). Cross-sectional images of the AV loop demonstrate continuous microfil perfusion at the site of anastomosis on day 5 (**h**) and prominent sprouting vessels by day 28 (**i**)

establishment and explantation is considerably smaller and therefore associated with significantly reduced donor site comorbidities.

The AVL has emerged as a well-established model for tissue engineering in small and large animal models, with the objective of generating axially vascularized tissues [1]. A thorough understanding of angiogenesis and the prevention of hypoxic conditions in engineered constructs are vital for the success of tissue engineering and tissue transfer. Current studies indicate that both hypoxia and flow-induced angiogenesis play a significant role in this model [8, 12]. The advantage of the induction of angiogenesis and subsequent vascularization in AVL constructs is that even matrices of larger volumes can be generated that are completely permeated by blood vessels that ensure the oxygenation of the entire construct.

Vascularization of rat AVL constructs has been studied in the context of various endogenous matrix materials that can influence the onset, speed, and extent of angiogenesis [6]. For example, AVLs embedded in Matrigel together with fibroblasts showed first signs of vascularization 7 days after AVL generation and reached a plateau 7 days later [7], suggesting an earlier onset and higher speed of vascularization in comparison with the collagen elastin matrix employed here. In another study, the vascularization of a collagen glycosaminoglycan matrix was assessed 14 and 28 days post-AVL surgery and was directly compared to AVLs embedded in collagen elastin matrices [9]. Irrespective of the type of matrix, the number of vessels was substantially increased on day 28 in comparison with day 14 [9]. Vessel counts were significantly higher in collagen elastin matrices compared to collagen glycosaminoglycan matrices [9]. When implanted within empty isolation chambers, rat AVLs produce their own endogenous matrix from fibrin-rich plasma exudates [3]. In this context, sprouting starts between day 3 and day 7 and reaches a maximum between days 14 and 21,

before slightly regressing afterwards with a clear reduction at day 28 [4]. These findings indicate that vascularization of endogenous fibrin matrices is induced earlier and progresses slightly faster in comparison with the collagen elastin matrix that we employed.

In conclusion, both the onset and the kinetics of vascularization seem to slightly differ depending on the matrix material used. However, when interpreting the available data, it is important to bear in mind that while the onset of vascularization can be safely compared, the ability of matrix materials to retain their volume over time and divergent degrees of shrinkage may have an impact on the outcome of vessel counts per area. Indeed, we have previously shown that matrix materials can significantly differ in terms of volume retention [15]. Therefore, we normalized vessel counts to matrix volume (Fig. 1d). However, a similar normalization has not been carried out in all of the studies that have been published so far, leading to a possible bias when comparing data obtained with different matrix materials. Regardless of these considerations, our findings have specific ramifications for the application of collagen elastin-embedded AVLs. We detected the highest vessel counts at day 21 post-AVL and therefore believe that 21 days post-AVL generation represents the optimal time point for transplantation of the AVL construct as a free tissue flap in rats.

Several lines of evidence suggest that the vascularization of rat AVL constructs is driven by hypoxia [4, 7, 12]. Here, we found in the context of AVLs embedded in a collagen elastin matrix that hypoxia is robustly induced between day 5 and day 15 post-AVL surgery, and that the percentage of hypoxic cells remained constantly high from day 15 throughout until day 28. By contrast, in a study in which rat AVL constructs were embedded in fibroblast-containing Matrigel, hypoxic cells were already present at 3 days post-AVL generation, and hypoxia was most pronounced at day 7 but could no longer be observed 14 and 28 days after AVL surgery [7]. Similarly, in rat AVLs embedded in an endogenous fibrin matrix, hypoxic cells were evident from day 3 onwards, and hypoxia peaked at day 7 post-AVL generation. Hypoxia reduced progressively from day 14 onwards, and hypoxic cells were absent from the construct 28 days post-AVL surgery [4], a timepoint at which hypoxia was still at a plateau phase in our setting with MatriDerm as an exogenous matrix material. Thus, in comparison with endogenous fibrin or Matrigel matrices, hypoxia is induced later in the context of collagen elastin-embedded AVLs. This is in line with the observation that the onset of vascularization is delayed in collagen elastin matrices when compared with fibroblast-containing Matrigel matrices and endogenous fibrin matrices. In contrast to our observation that the proportion of hypoxic cells was above 20% on day 5 (Fig. 2e) and plateaued at more than 70% from day 15 onwards, only 10% of the cells in rat AVLs embedded in an exogenous fibrin matrix were hypoxic 14 days post AVL surgery [12]. Moreover, in comparison with fibrin matrices and Matrigel matrices, we observed a more pronounced and persistent hypoxia. This suggests that the kinetics and extent of hypoxia can differ significantly dependent on the matrix material used, which is consistent with the notion that the onset of vascularization is delayed, and that the speed of vascularization is reduced in the context of elastin collagen matrices.

Small avascular tissue engineering constructs become vascularized extrinsically after grafting. However, in this setting, the size of the constructs that can be successfully implanted is restricted. AVL constructs are considered to be superior in this regard, since the vasculature established within the construct before transplantation is associated with both a better blood supply after grafting, and also with the possibility of successfully grafting even larger constructs.

The pattern of vascularization of the AVL construct has been assumed to be dictated by the design of the chamber. While intrinsic vascularisation by sprouting of new vessels from the AV loop is observed in isolation chambers (e.g. [4, 5, 7, 8, 13]), a porous chamber design additionally allows a more immediate, extrinsic vascularization [25] via sprouting and ingrowth of vessels from the periphery of the chamber into its center [26]. In the context of porous chambers with a fibrin-hydroxyapatite/β-tricalcium phosphate matrix, extrinsic and intrinsic vascularization of rat AVL constructs occurred in parallel, with only minor differences in their respective extent [18]. In contrast to this observation, and also unlike descriptions of exclusively intrinsic vascularization in isolation chambers (e.g. [4, 5, 7, 8, 14]), we report here that vascularization of a closed isolation chamber was initially extrinsic, and that intrinsic sprouting only occurred secondarily. In our setting, intrinsic vascularization first initiated within the venous portion of the loop and the venous graft, and finally also started in the arterial portion of the loop. In line with the observation that new vessels first sprout from the venous portion of the loop, vascularization first originating from the venous graft has also been reported in the context of AVLs embedded in Matrigel together with fibroblasts [7]. Another study followed the events during vascularisation of rat AVL constructs embedded in an exogenous fibrin matrix 2, 7, 10, and 14 days post-AVL surgery, with the explicit aim of assessing potential differences in vascularization emanating from the arterial and venous portions of the loop as well as from the venous graft [14]. Newly formed vessels were present on day 14, and the majority of the newly formed vessels were found to sprout from the venous portion of the loop and from the venous graft, whereas the arterial part of the loop showed hardly any nascent vessels [14]. Further confirmation of the venous origin of the first newly formed vessels in rat AVL constructs comes from a study that observed that new sprouts extruding

from the femoral vein were visible before sprouts from the recipient artery were detectable [4]. This is in line with the observation that in loops that contained an arterial instead of a venous graft, sprouting did not occur at all [8].

Together, these observations indicate that collagen elastin matrices support a different pattern of vascularization in AVL constructs, as extrinsic sprouting occurred even when closed isolation chambers were used.

In conclusion, our findings emphasize the critical role of the matrix utilized within the AVL construct concerning vascularization and hypoxia, as well as the significance of chamber design. Further studies should concentrate on the evaluation of longitudinal vascularization in different chamber designs to determine the optimal time point for transplantation of individualized engineered tissue flaps.

Acknowledgements The authors thank Kevin Krauth (KIT) for his help and support with the Teflon chamber design and Michael Wachter (KIT) for manufacturing the chambers. We gratefully acknowledge the expert technical assistance of Annette Gruber, Elena Tripel, and Daniel Strelzov.

Author Contribution NH designed and performed experiments, analyzed and interpreted data, prepared the figures, and wrote the manuscript. BT and FF supervised experiments and edited the manuscript. MS were involved in planning and supervised the work. SM contributed to the design and analysis of micro-CT scans and implementation of the research. MJ developed the protocol of micro-CT scans and performed the scans. BKG designed experiments and reviewed the manuscript. AD performed parts of the pathological analysis and interpreted the results. VJS devised the project and the main conceptual ideas. JPS and UK devised the main conceptual ideas of the study, reviewed the results, and approved the final version of the manuscript. WT interpreted data and wrote the manuscript. All authors reviewed the manuscript.

Funding Open Access funding enabled and organized by Projekt DEAL. NH is funded by the Clinician Scientist Program of Heidelberg University, Faculty of Medicine.

Data Availability The datasets generated and analyzed during the current study are available from the corresponding author on request.

Declarations

Ethical Approval The animal studies were performed after receiving approval of the local regulatory authorities (license numbers: 23 177–07/G13-7–008 and 23 177–07/G15-7–021).

Informed Consent On behalf of all authors, the corresponding author states that informed consent was obtained from all participants involved in the study.

Human and Animal Rights On behalf of all authors, the corresponding author affirms that human and animal rights were upheld in the study.

Competing interests The authors declare no competing interests.

References

1. Leibig N, Wietbrock JO, Bigdeli AK, Horch RE, Kremer T, Kneser U, et al. Flow-induced axial vascularization: the arteriovenous loop in angiogenesis and tissue engineering. Plast Reconstr Surg. 2016;138:825–35. https://doi.org/10.1097/PRS.0000000000002554.
2. Erol OO, Sira M. New capillary bed formation with a surgically constructed arteriovenous fistula. Plast Reconstr Surg. 1980;66:109–15. https://doi.org/10.1097/00006534-198007000-00021.
3. Mian R, Morrison WA, Hurley JV, Penington AJ, Romeo R, Tanaka Y, et al. Formation of new tissue from an arteriovenous loop in the absence of added extracellular matrix. Tissue Eng. 2000;6:595–603. https://doi.org/10.1089/10763270050199541.
4. Lokmic Z, Stillaert F, Morrison WA, Thompson EW, Mitchell GM. An arteriovenous loop in a protected space generates a permanent, highly vascular, tissue-engineered construct. FASEB J. 2007;21:511–22. https://doi.org/10.1096/fj.06-6614com.
5. Lokmic Z, Thomas JL, Morrison WA, Thompson EW, Mitchell GM. An endogenously deposited fibrin scaffold determines construct size in the surgically created arteriovenous loop chamber model of tissue engineering. J Vasc Surg. 2008;48:974–85. https://doi.org/10.1016/j.jvs.2008.05.021.
6. Cassell OC, Morrison WA, Messina A, Penington AJ, Thompson EW, Stevens GW, et al. The influence of extracellular matrix on the generation of vascularised, engineered, transplantable tissue. Ann N Y Acad Sci. 2001;944:429–42. https://doi.org/10.1111/j.1749-6632.2001.tb03853.x.
7. Hofer SO, Mitchell GM, Penington AJ, Morrison WA, Romeo-Meeuw R, Keramidaris E, et al. The use of pimonidazole to characterise hypoxia in the internal environment of an in vivo tissue engineering chamber. Br J Plast Surg. 2005;58:1104–14. https://doi.org/10.1016/j.bjps.2005.04.033.
8. Schmidt VJ, Hilgert JG, Covi JM, Leibig N, Wietbrock JO, Arkudas A, et al. Flow increase is decisive to initiate angiogenesis in veins exposed to altered hemodynamics. PLoS ONE. 2015;10:e0117407. https://doi.org/10.1371/journal.pone.0117407.
9. Schmidt VJ, Wietbrock JO, Leibig N, Gloe T, Henn D, Hernekamp JF, et al. Collagen-elastin and collagen-glycosaminoglycan scaffolds promote distinct patterns of matrix maturation and axial vascularization in arteriovenous loop-based soft tissue flaps. Ann Plast Surg. 2017;79:92–100.
10. Henn D, Chen K, Fischer K, Rauh A, Barrera JA, Kim YJ, et al. Tissue engineering of axially vascularised soft-tissue flaps with a poly-(ε-caprolactone) nanofiber-hydrogel composite. Adv Wound Care (New Rochelle). 2020;9:365–77. https://doi.org/10.1089/wound.2019.0975.
11. Haslik W, Lumenta DB, Kamolz LP, Frey M. The use of a collagen-elastin matrix as dermal regeneration template for the treatment of full-thickness skin defects. Adv Wound Care. 2010;1:438–44. https://doi.org/10.1089/97819348540134.438.

12. Yuan Q, Bleiziffer O, Boos AM, Sun J, Brandl A, Beier JP, et al. PHDs inhibitor DMOG promotes the vascularization process in the av loop by hif-1a up-regulation and the preliminary discussion on its kinetics in rat. BMC Biotechnol. 2014;14:112. https://doi.org/10.1186/s12896-014-0112-x.
13. Watson O, Novodvorsky P, Gray C, Rothman AM, Lawrie A, Crossman DC, et al. Blood flow suppresses vascular notch signalling via dll4 and is required for angiogenesis in response to hypoxic signalling. Cardiovasc Res. 2013;100:252–61. https://doi.org/10.1093/cvr/cvt170.
14. Polykandriotis E, Tjiawi J, Euler S, Arkudas A, Hess A, Brune K, et al. The venous graft as an effector of early angiogenesis in a fibrin matrix. Microvasc Res. 2008;75:25–33. https://doi.org/10.1016/j.mvr.2007.04.003.
15. Falkner F, Mayer SA, Heuer M, Brune J, Helt H, Bigdeli AK, et al. Comparison of decellularised human dermal scaffolds versus bovine collagen/elastin matrices for engineering of soft-tissue flaps. Plast Reconstr Surg. 2024;153:130–41. https://doi.org/10.1097/PRS.0000000000010511.
16. Wolf I, Vetter M, Wegner I, Böttger T, Nolden M, Schöbinger M, et al. The medical imaging interaction toolkit. Med Image Anal. 2005;9:594–604. https://doi.org/10.1016/j.media.2005.04.005.
17. Hahn HM, Jeong KS, Park MC, Park DH, Lee IJ. Free-flap transfer for coverage of transmetatarsal amputation stump to preserve residual foot length. Int J Low Extrem Wounds. 2017;16:60–5. https://doi.org/10.1177/1534734616689508.
18. Kozusko SD, Liu X, Riccio CA, Chang J, Boyd LC, Kokkalis Z, et al. Selecting a free flap for soft tissue coverage in lower extremity reconstruction. Injury. 2019;50:32–9. https://doi.org/10.1016/j.injury.2019.10.045.
19. Beier JP, Horch RE, Kneser U. Bilateral pre-expanded free TFL flaps for reconstruction of severe thoracic scar contractures in an 8-year-old girl. J Plast Reconstr Aesthet Surg. 2013;66:1766–9. https://doi.org/10.1016/j.bjps.2013.04.001.
20. Vogt PM, Steinau HU, Spies M, Kall S, Steiert A, Boorboor P, et al. Outcome of simultaneous and staged microvascular free tissue transfer connected to arteriovenous loops in areas lacking recipient vessels. Plast Reconstr Surg. 2007;120:1568–75. https://doi.org/10.1097/01.prs.0000282102.19951.6f.
21. Meyer A, Goller K, Horch RE, Beier JP, Taeger CD, Arkudas A, et al. Results of combined vascular reconstruction and free flap transfer for limb salvage in patients with critical limb ischemia. J Vasc Surg. 2015;61:1239–48. https://doi.org/10.1016/j.jvs.2014.12.005.
22. Chang EI, Chang EI, Soto-Miranda MA, Zhang H, Nosrati N, Robb GL, et al. Comprehensive analysis of donor-site morbidity in abdominally based free flap breast reconstruction. Plast Reconstr Surg. 2013;132:1383–91. https://doi.org/10.1097/PRS.0b013e3182a805a3.
23. Reichenberger MA, Harenberg PS, Pelzer M, Gazyakan E, Ryssel H, Germann G, et al. Arteriovenous loops in microsurgical free tissue transfer in reconstruction of central sternal defects. J Thorac Cardiovasc Surg. 2010;140:1283–7. https://doi.org/10.1016/j.jtcvs.2010.05.019.
24. Cavadas PC. Arteriovenous vascular loops in free flap reconstruction of the extremities. Plast Reconstr Surg. 2008;121:514–20. https://doi.org/10.1097/01.prs.0000297634.53915.e5.
25. Cassell OC, Hofer SO, Morrison WA, Knight KR. Vascularisation of tissue-engineered grafts: the regulation of angiogenesis in reconstructive surgery and in disease states. Br J Plast Surg. 2002;55:603–10. https://doi.org/10.1054/bjps.2002.3950.
26. Arkudas A, Pryymachuk G, Beier JP, Weigel L, Körner C, Singer RF, et al. Combination of extrinsic and intrinsic pathways significantly accelerates axial vascularization of bioartificial tissues. Plast Reconstr Surg. 2012;129:55e–65e. https://doi.org/10.1016/j.ebiom.2016.09.016.